



OPEN

Actively Targeted *In Vivo* Multiplex Detection of Intrinsic Cancer Biomarkers Using Biocompatible SERS Nanotags

SUBJECT AREAS:
BIOSENSORS
PRE-CLINICAL STUDIESU. S. Dinish^{1*}, Ghayathri Balasundaram^{1*}, Young-Tae Chang^{1,2} & Malini Olivo^{1,3}Received
7 October 2013Accepted
27 January 2014Published
12 February 2014Correspondence and
requests for materials
should be addressed to
M.O. (malini_olivo@
sbic.a-star.edu.sg)* These authors
contributed equally to
this work.

¹Singapore Bioimaging Consortium, Agency for Science Technology and Research (A*STAR), 11 Biopolis Way, Singapore 138667, ²Department of Chemistry & MedChem Program of Life Sciences Institute, National University of Singapore, 117543 Singapore, ³School of Physics, National University of Ireland Galway, Galway, Ireland.

Surface-enhanced Raman scattering (SERS) technique is becoming highly popular for multiplex biosensing due to the 'fingerprint' Raman spectra from every molecule. As a proof-of-concept, we demonstrated the actively targeted multiplex *in vitro* and *in vivo* detection of three intrinsic cancer biomarkers - EGFR, CD44 and TGF β RII in a breast cancer model using three multiplexing capable, biocompatible SERS nanoparticles/nanotags. Intra-tumorally injected antibody conjugated nanotags specifically targeting the three biomarkers exhibited maximum signal at 6 hours and no detectable signal at 72 hours. However, nanotags without antibodies showed no detectable signal after 6 hours. This difference could be due to the specific binding of the bioconjugated nanotags to the receptors on the cell surface. Thus, this study establishes SERS nanotags as an ultrasensitive nanoprobe for the multiplex detection of biomarkers and opens up its potential application in monitoring tumor progression and therapy and development into a theranostic probe.

Among the various molecular imaging techniques for biomedical applications, optical techniques have gained great popularity due to the inherent advantages such as the improved spatial resolution, non usage of radioactive probes and higher sensitivity¹. Surface Enhanced Raman Scattering (SERS) is recently being explored as an effective molecular imaging optical modality for various pre-clinical biomedical applications due to its inherent ability to generate enhanced Raman spectra of analyte when it is in close proximity to nano-roughened noble metal surfaces like silver (Ag) or gold (Au)²⁻⁵. SERS provides for biomedical research the most promising advantages like multi-parameter molecular analyses and multiplexing potential, which are due to the narrow 'fingerprint' Raman spectra unique to the chemical species. These characteristic enhanced Raman spectra from a particular molecular species can be clearly used to identify and also to quantify different targets in a mixture.

Early detection is the most effective means of improving prognosis for many fatal diseases such as cancer. In most cases, simultaneous detection of multiple biomarkers at early stage provides an added advantage in increasing the diagnostic accuracy and treatment response monitoring. The most commonly used fluorescence methods often fail in multiplex detection owing to their broad emission spectrum that leads to spectral overlapping and strong background auto-fluorescence⁶⁻⁸. In this context, recently, SERS is being proposed as an alternative and it is realized through SERS-active nanoparticles (SERS nanotags)⁹⁻¹². SERS nanotags are constructed by attaching strong Raman active molecules (reporter molecules, RMs) onto Au nanoparticles (AuNPs) and encapsulating them in a polyethylene glycol (PEG)/Silica/bovine serum albumin shell¹³⁻¹⁷. This encapsulation helps in providing the physical robustness, stable signal, protection from bio-chemical environment and means for bio-conjugation. These nanotags can be easily functionalized with various receptor moieties for specific and active *in vivo* targeting of biomarkers. Such bioconjugated mono-disperse nanotags produce strong and unique SERS signal to be monitored for multiplex detection. SERS nanotags possess many significant advantages over fluorescence based NPs like quantum dots such as (i) multiplex detection capability due to spectral fingerprinting, (ii) not being susceptible to photo-bleaching and (iii) low cytotoxicity due to the usage of AuNPs^{9,13,14,18,19}.

The most crucial aspect when developing a SERS nanotag is the choice of the Raman molecule because the sensitivity of the probe for biosensing primarily depends on the signal intensity generated by RM. To address this, recently, a library of near infra-red (NIR) active RMs were developed and successfully demonstrated for *in vivo* detection of cancer biomarker¹⁶. To enhance the sensitivity of SERS nanotags for *in vivo* application, plasmonic tuning of SERS substrates (nanoparticles) have also been demonstrated. This is achieved by constructing the SERS



nanotags with metallic NPs in the form of nanorods^{20–22}, hollow nanostructures^{1,17,23,24}, Nanostars²⁵ and nanoflowers²⁶ to create NIR-active hot spots.

Recently, SERS nanotags have been successfully used for the detection of cancer biomarkers^{12,14–16,27–29}. *In vitro* multiplex detection of biomarkers in cell lines and tissue samples using SERS nanotags constructed with commercial reporter molecules is also studied^{25,30,31}. Simultaneous *in vitro* evaluation of p53 and p21 expression level for early cancer diagnosis is also demonstrated using multiplexing capable SERS nanotags²². SERS nanotag based passive targeted multiplexing is established in a mouse model using commercial nanotags⁹. In this case, successful multiplex detection of ten nanotags (for subcutaneously administered) and accumulation of five different nanotags in liver (for intravenously injected) are monitored. Recently, *in vivo* detection of single biomarker was achieved using three different SERS nanotags constructed with NIR active reporter molecules¹⁰. NIR active SERS nanotags constructed with Au/Ag hollow shell and standard RMs are also demonstrated for the passive *in vivo* multiplex detection when they are subcutaneously injected⁴. SERS nanotag constructed with Au nanorods was successfully employed for the *in vivo* cancer detection and photothermal therapy²⁰. They also demonstrated the multiplex detection using subcutaneously injected non bioconjugated nanotags. Recently, biocompatibility of SERS nanotags in zebra fish embryo was studied and later two SERS nanotags was injected directly into the embryo and monitored its distribution³². In another study, multiplex *in vivo* SERS imaging was carried out to quantitatively correlate the concentration of four different non bio-conjugated nanotags, which were injected subcutaneously on the dorsum of a nude mouse³³. Recently, the fabrication and characterization of a fiber optic-based Raman endoscope system that has the capability to detect and quantify the presence of single or multiplexed SERS nanoparticles was developed. In this study, the usability and capability of the developed Raman endoscope system to detect and multiplex an array of SERS nanotags within a phantom model and on excised tissue sample was performed³⁴.

In most of the reported studies for *in vivo* detection, main focus was directed towards the sensing of passively targeted non bioconjugated nanotags. However, the real challenge lies in the *in vivo* multiplex detection of actively targeted biomarkers, which has the clinical relevance. In this context, as a proof-of-concept, we demonstrated the targeted multiplex detection of intrinsic cancer biomarkers - EGFR, CD44 and TGF beta receptor II (TGFβRII) in MDA-MB-231 breast cancer cell line that expresses these receptors on their surface and murine xenograft model using three multiplexing capable and biocompatible SERS nanotags constructed with RMs, Cyanine 5 (Cy5), malachite green isothiocyanate (MGITC) and rhodamine 6G (Rh6G) that were conjugated to antibodies against these biomarkers. EGFR is the cell-surface receptor for members of the epidermal growth factor (EGF) family of extracellular protein ligands. It is a prognostic marker in many types of cancer including breast cancer³⁵. CD44 is a major cell surface adhesion molecule and is a receptor for the glycosaminoglycan, hyaluronan (HA). It plays an important role in tumor growth and metastasis³⁶. TGFβRII is the receptor for the anti-proliferative TGFβ ligand. Down regulation of TGFβRII is a key step in breast carcinogenesis and worsens the prognosis³⁷. In this study, we demonstrated the multiplex detection of intrinsic cancer markers *in vitro* and *in vivo* in a xenograft model and their longer retention in the tumor after intra-tumoral injection. We chose the route of direct intra-tumoral injection because previous extensive studies showed that it results in increased accumulation of the drug/particle at the tumor site than any other organ and lesser dissipation to other healthy organs^{38–43} compared to intravenous injection that result in lesser accumulation at the tumor site and wide distribution throughout the body^{42,43}. We believe that this demonstration of the actively targeted *in vivo* multiplex detection of cancer biomarkers using SERS nanotags has the

potential to be used for ultrasensitive biosensing and molecular imaging applications to monitor various molecular markers *in vivo*.

Results

Characterization of SERS nanotags. Absorption spectrum of pure AuNPs, SERS nanotags and antibody conjugated SERS nanotags are shown in supplementary information (SI, Fig S1). The absorption spectrum of SERS nanotags resembles that of AuNP, suggesting the stable encapsulation without causing aggregation of the nanoparticles. For antibody conjugation, the heterofunctional PEG was covalently conjugated with the free amine functional group of antibody through EDC-NHS coupling and the bioconjugation of antibody to the nanotag can be confirmed by the protein absorption peak at ~280 nm in the spectra^{14,15,44–46}.

TEM images of the Pure Au NPs, MGITC, Cy5 and Rh6G SERS nanotags are shown in Fig. 1 (A–D). It can be seen that all the three nanotags are predominantly mono-disperse with minimal aggregation. Mono-dispersivity of the nanotag is highly crucial when using it for sensing applications. Aggregation can cause fluctuation in SERS intensity, which is not ideal for *in vivo* sensing applications. The PEG encapsulation will help in minimizing the aggregation along with providing a stable encapsulation layer for the RMs. It was also confirmed that after PEG encapsulation and bioconjugation, the morphology of the particles remained intact with an average diameter of ~60 nm.

SERS properties of these nanotags were studied at 785 nm laser excitation. At the same experimental conditions, the characteristic multiplexing peaks of Cy5 and MGITC nanotags possess similar SERS intensity while that of Rh6G nanotag has about only half the intensity of the former two (Fig. S2, SI). This difference is attributed to the inherent Raman cross section associated with the RMs. We modified the Cy5 reporter molecule by lipoic acid (LA) linker so that the molecule can chemisorb on to AuNPs by thiol chemistry⁴⁷. This will help in forming strong covalent bond to AuNPs, which can help in providing better SERS intensity. In the case of MGITC, chemically relatively weak Au-SCN interaction is the main binding force, while Rh6G molecules can only physisorb on to AuNPs. As shown in Fig. 1E, it is clear that these three nanotags are ideal candidates for multiplex detection as they possess clearly distinguishable peaks in 1000–1700 cm⁻¹ spectral range. In this study, the characteristics peak for Cy5 nanotag at 1120 cm⁻¹, MGITC at 1175 cm⁻¹ and Rh6G at 1650 cm⁻¹ were monitored for targeted multiplex detection of biomarkers. SERS intensity of the multiplexing peaks from each bioconjugated nanotag was studied over a period of three weeks to establish the stability of the nanotags (Fig. S3, SI).

Western blot analysis and cell viability of SERS nanotags. MDA-MB-231 breast cancer cell line has been known to express a variety of cell surface receptors including the three cancer biomarkers -EGFR, CD44 and TGFβRII. To determine the expression levels of these proteins, western blot was performed on two different concentrations of total protein extracted from cultured MDA-MB-231 cells. All three proteins showed detectable levels of expression with EGFR (132 kDa) being highly expressed, CD44 (82 kDa) being second highly expressed while TGFβRII (68 kDa) being lowly expressed compared to the other two (Fig. 2A). The full blots of the cropped images represented here are given in Fig. S4 in SI. For targeted SERS detection of these biomarkers, each of the nanotags was appropriately conjugated to the antibodies against these proteins. For instance, EGFR with highest expression was linked to Rh6G nanotag having least SERS signal while CD44 and TGFβRII with lesser expression levels were conjugated respectively to MGITC and Cy5 with relatively higher SERS signal.

Before introducing the SERS nanotags into cells or animals, their cytotoxicity was assessed on MDA-MB-231 cells. Appropriate amounts of AuNPs, SERS nanotags with and without antibody

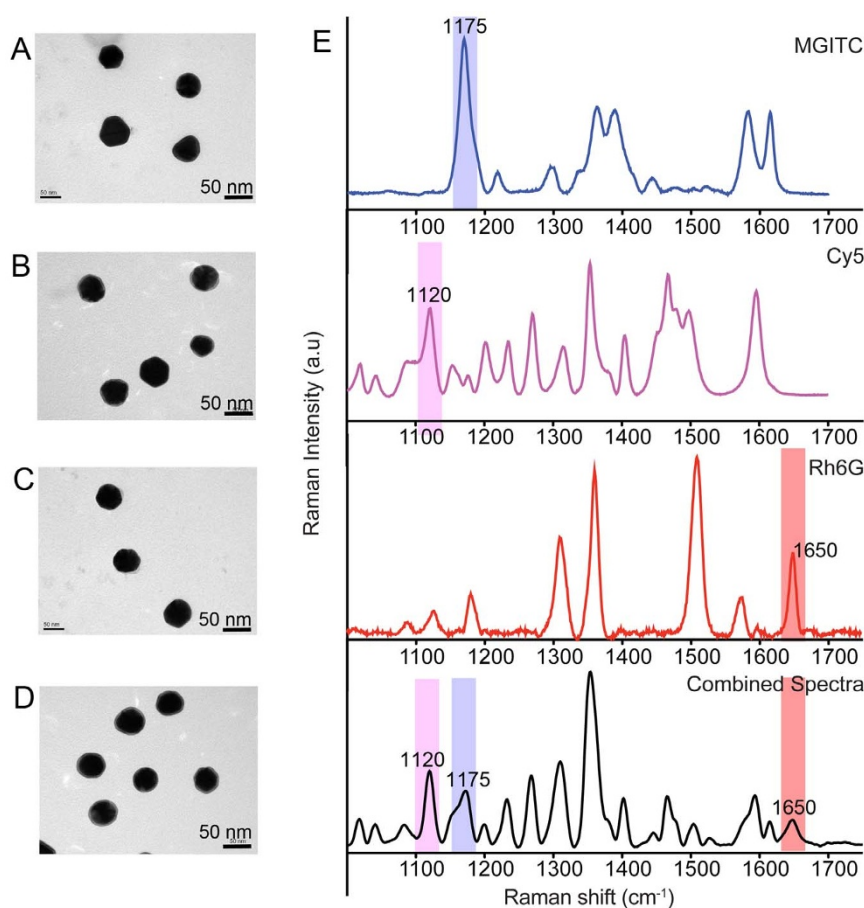


Figure 1 | (A–D) TEM image of the pure AuNPs, SERS nanotags with MGITC, Cy5 and Rh6G reporter molecules respectively. (E) SERS spectra of individual SERS nanotags and its mixture depicting their multiplexing peaks. The most distinctive multiplex peak from each reporter is marked.

bionconjugation were incubated with the cells for three hours and cell viability was measured after 24 hours. AuNPs treated cells exhibited almost 100% viability. While AuNPs coated with Cy5 and MGITC either conjugated or not conjugated to antibodies exhibited cell viability of more than 95%, AuNPs coated with Rh6G, both conjugated and not conjugated to antibodies exhibited a cell viability of around 85% (Fig. 2B). This could be because of the general toxicity of rhodamine dyes. Rh6G, because of its lipophilic - cationic nature, are known to selectively kill carcinoma cells of epithelial origin⁴⁸. Lesser cytotoxicity observed in this case indicated the biocompatibility of SERS nanotags.

Multiplex detection of biomarkers *in vitro*. After confirming the presence of the three biomarkers - EGFR, CD44 and TGF β RII in the MDA-MB-231 cell line using western blot, the cells were exposed to a mixture of three antibody conjugated SERS nanotags (Rh6G-EGFR, MGITC-Cd44 and Cy5-TGF β RII) to map the biomarkers using SERS. Multiplexed SERS spectra measured from the cell surface is provided in Fig. 3A, while the bright field image of the cells are shown in Fig. 3B. It is obvious that the point spectral measurement from the cell surface clearly indicates the ‘fingerprint’ spectral peak from each of the three nanotags that allows for the multiplex detection of biomarkers. Relative distribution of the intrinsic cancer biomarkers on the cell surface was obtained by mapping at respective Raman peaks of the SERS nanotag that the antibody to the biomarker is attached to. Fig. 3(C–E) confirm the specific interaction and binding of the bioconjugated nanotags to the three biomarkers on the cell surface. Intensity mapping at 1120 cm^{-1} (Cy5) demonstrated the localization of the antibody conjugated Cy5 and thus the distribution of TGF β RII. Similarly, the intensity mapping at

1175 cm^{-1} and at 1650 cm^{-1} demonstrated the localization of antibody conjugated MGITC and Rh6G nanotags and hence the distribution of CD44 and EGFR respectively. To test the specificity of the antibody conjugated SERS tags, SERS mapping was done on Jurkat cells (that do not express EGFR, CD44 and TGF β RII) exposed to the same mixture of SERS nanotags. SERS images obtained from these cells were dark with few bright (Fig. S5, SI) spots unlike the MDA-MB-231 cells indicating that the tags did not bind to the cell surface because of the absence of the receptors.

To validate the binding of the tags to the cell surface, Raman mapping was carried out for all three tags at a depth interval of 2.5 μm . A representative image stack mapped for Cy5 nanotag conjugated to TGF β RII is provided in Fig. 3F. Similarly, depth scan image for the MGITC and Rh6G nanotags are provided in Fig. S6 (SI). At deeper depth of the cell ($\sim 10 \mu\text{m}$), no SERS intensity was detected. This is an indication that the nanotags are bound to the cell surface that produced the signal as in Fig. 3 (C–E). This aspect was also validated using dark field imaging of MDA-MB-231 cells exposed to antibody conjugated and non-conjugated SERS nanotags. (Fig. S7, SI). The antibody conjugated SERS nanotags bound to the biomarkers (EGFR, CD44 and TGF β RII), which are cell membrane bound receptors, to give strong bright scattering spots on the cell surface. These bright spots are due to the light scattering property of the AuNPs in the bound nanotags. However, non-conjugated nanotags did not bind to cell surface and thus no bright scattering spots were observed. Detailed descriptions of this experiment are provided in SI. Another set of SERS mapping images of the cell using three nanotags is provided in Fig. S8 (SI).

EGFR is the founding cell surface receptor of the erbB family of receptors that help in the growth of cells upon binding of a subset of

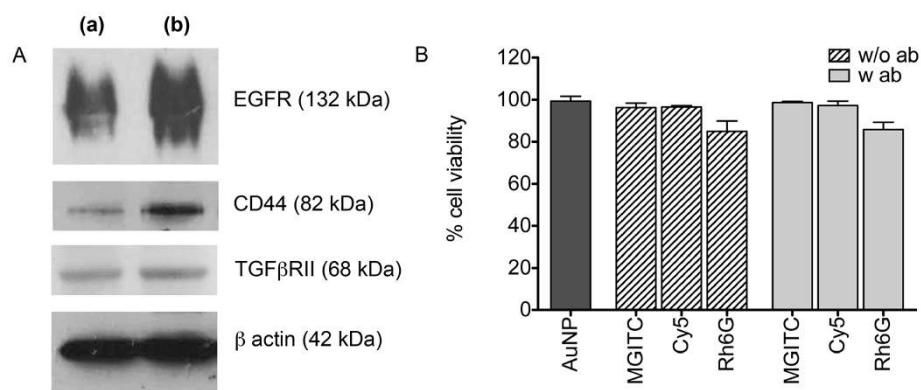


Figure 2 | (A) Confirmation of the expression of intrinsic biomarkers-EGFR, CD44 and TGF β R II in 10 (a) and 15 μg (b) of total protein extracted from cultured MDA-MB-231 by western blot. Total proteins from MDA-MB-231 cells were electrophoresed under same experimental conditions and probed for β -actin, CD44 and TGF β R II proteins using respective primary antibodies followed by corresponding secondary antibodies. EGFR was detected by electrophoresing total proteins in SDS free conditions followed by probing using corresponding primary and secondary antibodies. (B) Cell viability study using Cell Counting Kit-8 on MDA-MB-231 cells exposed to pure AuNP, antibody-bioconjugated (w ab) and non bioconjugated (w/o ab) SERS nanotags (MGITC, Cy5 and Rh6G) after 24 hours.

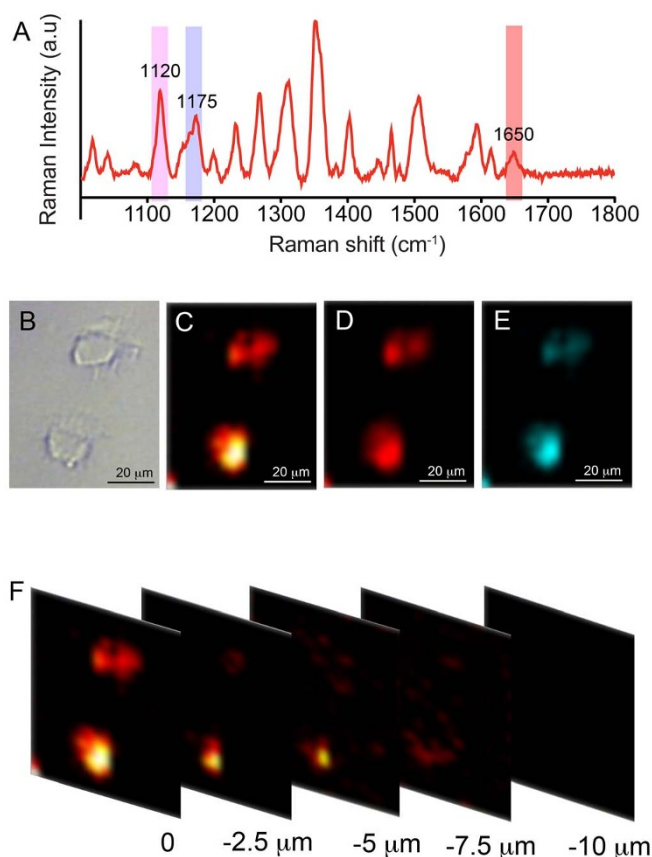


Figure 3 | *In vitro* SERS mapping results with three SERS nanotags. (A)-SERS spectra from the cell depicting the multiplexing peak from each nanotag bound to corresponding biomarker on the cell surface and (B)-bright field image of the cell. (C-E) shows the SERS intensity map image demonstrating the expression and relative distribution of the biomarkers-TGF β R II , CD44 and EGFR on the cell surface bound to the antibody conjugated SERS nanotags, Cy5, MGITC and Rh6G respectively. SERS mapping was carried out at 1120 cm^{-1} peak of Cy5, 1175 cm^{-1} of MGITC and 1650 cm^{-1} of Rh6G. (F) SERS intensity map images of the z-series scan at different depth for the Cy5 nanotag (bound to TGF β R II biomarker). Mapping was carried out at a depth interval of 2.5 μm .

ligands. Overexpression of EGFR has been associated with a number of cancers for which prognosis is poor³⁵. CD44 is a multistructural and multifunctional cell surface molecule involved not only in many physiological activities of normal cells but also pathologic activities of cancer cells. It is overly expressed in breast cancer stem cells and is implicated in tumorigenesis and metastasis and thus it is a widely accepted marker for breast cancer stem cells³⁶. TGF β R II is a cell surface receptor that transmits signals from the outside to the inside of the cell mostly to inhibit cell growth and division. Because of this, TGF β R II is considered as a tumor suppressor and down regulation of the same worsens the prognosis of several carcinomas³⁷. Simultaneous multiplex detection of these three biomarkers has great significance in the cancer prognosis. In this context, the proof-of-concept study of the simultaneous detection of the biomarkers that we demonstrated here could find tremendous potential in increasing the sensitivity and diagnostic accuracy of a variety of cancers and other disorders.

***In vivo* multiplex detection.** We carried out the multiplex detection of intrinsic biomarkers *in vivo* by injecting 200 μl of the three bioconjugated SERS nanotags (MGITC, Cy5 and Rh6G in the ratio 1 : 1 : 2) into the centre of the tumor on a subcutaneous MDA-MB-231 breast cancer xenograft mouse model (Fig. 4A). SERS nanotags conjugated to antibodies served as test formulation while non-conjugated nanotags served as control formulation. SERS measurements were taken at regular intervals starting immediately after the injection. The spectra clearly revealed the distinct Raman peaks corresponding to each of the three nanotags from both the control and test mice with least spectral overlap in the 1000–1800 cm^{-1} region (Fig. 4B and 4C). Raman shift at 1120 cm^{-1} , 1175 cm^{-1} and 1650 cm^{-1} corresponds to the Cy5, MGITC and Rh6G respectively.

Fig. 5 shows the variation in detected SERS intensity of each nanotag as function of time. At 0th hour (immediately after the injection), both test and control mice had least signals from all three tags after which the signals started to increase in both cases. For control mice, SERS signals increased only up to 1st hour after which it started to decrease at 4th hour and at 6th hour signal was weak. At 24th hour, no SERS signal from any nanotag could be detected. On the other hand, for the test mice, SERS signals increased and reached a maximum at \sim 6 hours after which it decreased slightly up to 24 hours. At 48 hours, there was a considerable decrease in intensity with no detectable signal at 72 hours. The lower signal intensity for Rh6G nanotag in all the cases is attributed to its inherent lower Raman cross section. At all time points, multiple measurements were carried out

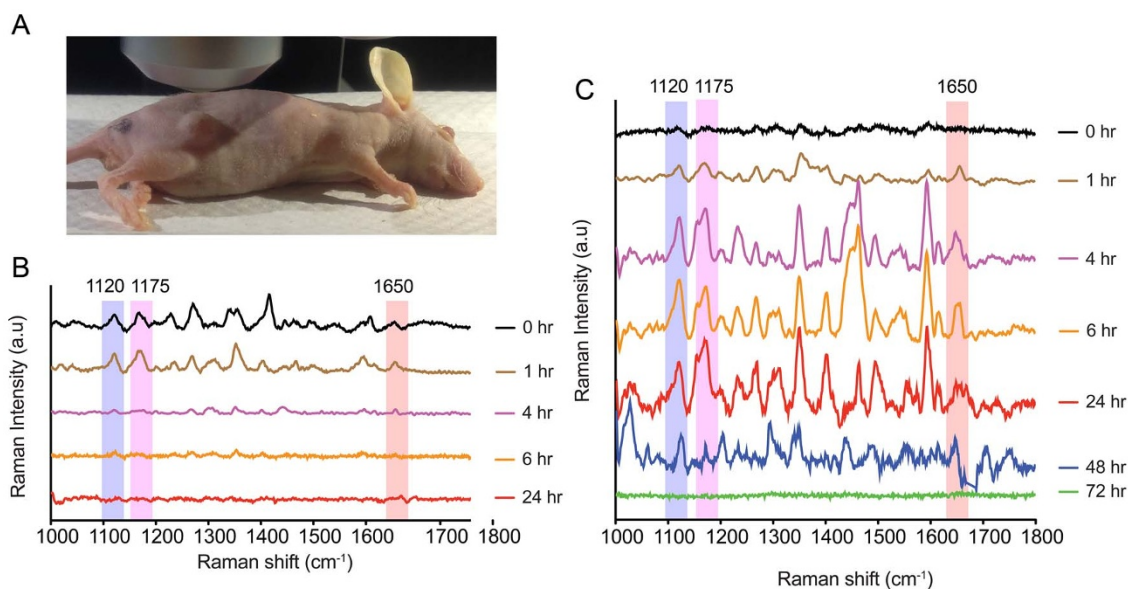


Figure 4 | *In vivo* multiplex detection in xenograft tumor: (A):- Image of a tumor bearing mouse from test group used in experiment. (B):-SERS spectra from tumor site in a representative control mice showing the peaks at 1120,1175 and 1650 cm^{-1} from non bioconjugated SERS nanotags corresponding to Cy5, MGITC and Rh6G respectively. Signal intensity is not detectable 6 hours after injection and nanotags gets cleared fast from the body due to the lack of specific binding. (C):- SERS spectra from tumor site in a representative test mice showing the peaks at 1120, 1175 and 1650 cm^{-1} from the bioconjugated Cy5, MGITC and Rh6G nanotags bound to TGF β RII, CD44 and EGFR biomarker respectively. Due to active targeting, multiplex SERS spectra is observed up to 48 hours followed by the clearance of nanotags from the mouse body by ~ 72 hours.

different tumor locations on a total of six animals for test and control. The difference in the SERS intensity could be attributed to the specific targeting of the antibody conjugated nanotags in the test mice. The antibodies in the test group bound strongly to their corresponding cell surface receptors in the tumor, thus enabling the SERS spectra from these tags to be detected for a longer time. However, in the control group, because of the absence of targeting antibodies, SERS nanotags dissipated from the tumor site quite fast.

Generally, NPs of size around 60 nm are cleared by the cells in the liver and spleen⁴⁹. In this scenario, subsequently, we measured the SERS signals from liver and spleen to understand the clearance of the nanotags in the mice. We found that SERS signal could hardly be detected in the liver and spleen. Upon intra-tumoral injection, percentage of nanoparticle accumulation per organ was higher for tumor than that in liver, spleen, kidney or any other organ unlike

in intravenous injection where percentage of nanoparticle accumulation per organ was greater in spleen, liver and kidney followed by tumor^{43,50}. It is difficult to detect the SERS signal from this lesser percentage of nanoparticle accumulated in the liver and spleen unless the SERS nanotags (which in our case had their absorption maximum in the visible region) in this study are excited by a laser source that matches with their absorption maximum. This type of SERS is called Surface Enhanced Raman Resonance Scattering (SERRS) where the wavelength of the laser source resonates with the absorption maximum of the reporter molecule to give an enhancement in the signal by 1–2 orders magnitude. Those small amounts of nanotags reaching the liver or spleen might have been excreted through the fecal pathway. Some of them that managed to enter the blood stream would have been phagocytosed by the reticulo endothelial system, taken to the liver and excreted through the feces together with bile juice⁵¹.

Faster clearance from the body, target specificity and improved stability makes these nanotags efficient *in vivo* imaging/sensing probes. The unparalleled multiplexing capability makes these nanotags ideal nanoprobe for the simultaneous detection of multiple biomarkers in diseases like cancer, which has many markers to define each of its progressive stage. SERS nanotags constructed with Au nanorods, which has the longitudinal surface plasmon resonance in NIR range coupled with plasmonic heating associated photothermal property²⁰, can be employed in developing these particles as a sensitive theranostic probes. Such probes will find tremendous application in efficient cancer detection and therapy especially when SERS tags are administered to bind to multiple biomarkers on the cancer cells.

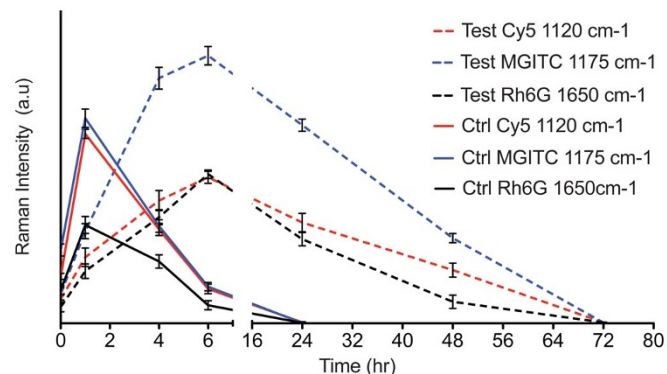


Figure 5 | Representation of the variation in SERS intensity of the three nanotags in test (dotted lines, with antibody conjugation) and control mice (Ctrl-solid lines, without antibody conjugation) *in vivo* at tumor site as a function of time. SERS intensity at 1120 cm^{-1} (for Cy5), 1175 cm^{-1} (for MGITC) and 1650 cm^{-1} (for Rh6G) were monitored over a period of 72 hours.

Discussion

SERS technique that exploits the unique inherent “fingerprint” Raman spectra from molecule is recently emerging as the most promising tool for *in vivo* biosensing and imaging. SERS nanotags having characteristics spectra that do not overlap with each other are starting to find extensive applications in simultaneous detection of multiple biomarkers *in vivo*. However, in most of the reported stud-



ies, the main focus had been on sensing of passively targeted non bio-conjugated nanotags^{1,9,32,33}. *In vivo* multiplex detection of actively targeted biomarkers, which is of clinical relevance has not been addressed before. Realizing this necessity and exploiting the multiplexing capability of SERS nanotags, we developed actively targeting SERS nanotags and demonstrated *in vitro* and *in vivo* actively targeted simultaneous detection of three intrinsic cancer biomarkers - EGFR, CD44 and TGFβRII using three biocompatible SERS nanotags constructed with common RMs such as Cy5, MGITC and Rh6G. SERS nanotags constructed with these RMs are ideal for multiplexing studies as it possess distinct Raman peaks in the 1000–1800 cm^{-1} . Moreover, these nanotags exhibited high cell viability and also great SERS signal stability over a period of three weeks. We observed that intra-tumorally injected antibody conjugated SERS nanotags showed SERS signal of all three nanotags up to two days whereas the SERS nanotags without antibodies showed detectable SERS signal up to only ~4–6 hours. SERS nanotags with antibodies specifically interacted and actively bound to their receptors and thus contributed to the prolonged signal at the tumor site whereas SERS nanotags without antibodies dissipated fast from the tumor site. This way, these tags can be used to quantify the levels of biomarkers and thus can be used to monitor the cancer progression or effectiveness of therapy. No detectable SERS signal was observed in the liver and spleen of animals injected with SERS tags with or without antibody. This served as an indication of their faster clearance from the body and hence their safety profile.

Early diagnosis of the disease is only possible if the detection of biomarkers is carried out at a very low concentration. Moreover, simultaneous detection of multiple biomarkers will be extremely beneficial for a fool proof diagnosis. It was reported that multiplex detection of biomarkers such as alpha fetoprotein (AFP) and alpha-1-antitrypsin (A1AT) will be extremely useful in the early diagnosis of hepatocellular carcinoma, where the average survival rate is only about 4 months after the onset of initial symptoms^{52,53}. In this context, this report on the simultaneous multiplex detection of intrinsic cancer biomarkers using antibody conjugated mixture of SERS nanotags can be efficiently used in the targeted ultrasensitive *in vivo* detection and imaging. Further, it may find promising applications in the early diagnosis of diseases and monitoring the effectiveness of the cancer therapy. Together with Au nanorods which have the longitudinal surface plasmon resonance in NIR range coupled with plasmonic heating, these SERS nanotags can be employed in targeted photothermal therapy to treat cancer. We believe that the excellent multiplexing capability, target specificity, faster clearance and improved stability of the SERS nanotags in combination with photothermal properties of metallic nanoparticles will open up a new regime in developing efficient theranostic probes for various biomedical applications.

Methods

Preparation of SERS nanotags. Three SERS nanotags were prepared from Raman reporter molecules-MGITC, Rh6G and Cy5. MGITC and Cy5 (10 μM) and Rh6G (50 μM) solutions were mixed with 60 nm AuNPs (BBInternational, 2.6 \times 10¹⁰ particles/mL) separately in 1 : 9 v/v ratio for 20 minutes. We modified the Cy5 reporter molecule by LA linker so that the molecule can chemisorb on to AuNPs by thiol chemistry⁴⁷. We employed PEG encapsulation for antibody conjugation and also for the protection of the nanotags. Thiolated-carboxylated PEG (HS-PEG-COOH, 10 uM, RAPP Polymere GmbH) was first added to the AuNP-Raman reporter conjugate and mixed for 20 minutes. Subsequently, thiolated PEG (PEG-SH, 10 uM, RAPP Polymere GmbH) was added to the mixture and incubated for 3 hours. Later, these solutions are centrifuged to remove the excess PEG and re-suspended in PBS. To achieve an effective antibody bioconjugation, carboxylic acid functional group on the surface of these PEG encapsulated NPs were activated by ethyl dimethylaminopropyl carbodiimide (EDC) and sulfo-N-hydroxysuccinimide (NHS) coupling reaction. To realize this, EDC (25 mM in water) and NHS (25 mM in water) were added to the PEG encapsulated nanotag and mixed for 20 minutes. The excess amount of EDC and NHS was removed by centrifugation and then the solutions are re-suspended in PBS. Finally, anti-EGFR antibody (100 μL , 200 $\mu\text{g}/\text{mL}$, Santa Cruz, sc-120) was reacted with activated Rh6G nanotag, anti CD44 antibody (100 μL , 200 $\mu\text{g}/\text{mL}$ EPR1013Y, Abcam) with MGITC and anti TGFβRII antibody (100 μL ,

200 $\mu\text{g}/\text{mL}$ ab61213, Abcam, Abcam) with Cy5 nanotag at 25°C for 2 hours and then kept for overnight incubation at 4°C. Finally, non-specifically bound antibodies were removed and the bioconjugated nanotags were stored at 4°C.

TEM and UV-Vis absorbance study. Transmission Electron Microscope (TEM) images were taken using Jeol JEM-1010 machine. Acceleration voltage was 40 ~ 100 KV and stability was 2 ppm min^{-1} . The magnification range of the instrument covers from 50 to 600,000 \times with a resolution of 0.3000 nm. Images of these PEG encapsulated nanotags were taken at a 250,000 \times magnification.

UV-Vis absorption spectra were obtained with Hitachi U-2900 spectrometer with a double-beam optical system and spectral bandpass of 1.5 nm.

Cell culture. Human metastatic breast cancer cell line MDA-MB-231 was maintained in RPMI supplemented with 10% fetal bovine serum (FBS) and 1% antibiotic - antimycotic solution. Human T cell leukemia cell line, Jurkat (clone E6-1) were maintained in RPMI medium supplemented with 10% FBS and 1% antibiotic - antimycotic solution. Cells were used for various assays at 80% confluency.

Western blot and cell viability assay. Cells were lysed using appropriate volumes of RIPA lysis buffer (Sigma-Aldrich), a mammalian cell lysis and protein solubilization reagent. Cell lysates were collected and clarified by centrifugation at 10,000 rpm for 10 minutes. Western Blotting was performed on clarified lysate with SDS-PAGE Gel electrophoresis system. Briefly, 10 μg and 15 μg of the protein samples were boiled with reducing sample buffer and electrophoresed on a 10% Tris gel with Tris running buffer; blotted on to PVDF membrane and subsequently probed with primary antibodies against CD44 (EPR1013Y, Abcam) and TGFβRII (ab61213, Abcam). For EGFR, 10 μg and 15 μg of the native protein samples were electrophoresed on a 10% Tris gel (with no SDS) with Tris running buffer (with no SDS) and blotted on to a PVDF membrane and subsequently probed with anti-EGFR antibodies (sc120, Santacruz). Horse radish peroxidase-conjugated anti-mouse whole IgG antibody (NA931-1ML, GE Healthcare, Milwaukee, WI) and anti-rabbit whole IgG antibody (NA934-1ML, GE Healthcare, Milwaukee, WI) were then added, and secondary antibodies were detected through autoradiography using enhanced chemiluminescence (ECL Plus, GE Healthcare).

For cell viability study, 1×10^4 cells were seeded per well in a 96 well plate. 100 μL of 1 OD unit of various SERS nanotag formulations with and without antibody conjugation were added in at least triplicates and incubated for 3 hours. After discarding the free nanotags, cells were replenished with complete RPMI, incubated for 24 hours and measured for cell viability using Cell Counting Kit - 8 (CKK-8, Sigma).

SERS spectral measurement and *in vitro* mapping. Spectral measurements of the SERS nanotags were measured using Raman microscope (Renishaw InVia) with 785 nm excitation laser and equipped with a grating (1200 lines/mm) having a spectral resolution of ~1.2 cm^{-1} . System was connected to the microscope (Leica) and a CCD detector cooled at -70°C. 20 μL of each SERS nanotag solution and mixture of the nanotags was pipetted onto a clean glass slide; a cover slip was placed on top of it and placed on the microscope stage for measurement. The laser light was coupled through 50 \times objective lens (Leica, NA 0.75), which was also used to collect the Stokes shifted Raman signal. The laser power at the sample was 1.2 mW. A notch filter was used to cut off the Rayleigh scattered light from the sample. The instrument was calibrated with Raman signal from a silicon standard at 520 cm^{-1} . Spectral acquisition, baseline correction and removal of fluorescence band in the spectra were performed using WIRE 3.2 software.

To perform the *in vitro* SERS mapping of cells treated with SERS nanotags, initially, 0.5×10^6 cells were seeded on a 22 \times 22 mm glass coverslip in a 6 well plate. SERS nanotags conjugated to the three antibodies were added to the cells and incubated for 3 hours. After removing free and unbound SERS nanotags, cells were fixed using 4% paraformaldehyde for 15 minutes. After washing with PBS, cover slips were mounted on a glass slide using Clear Mount with Tris Buffer mounting medium (Electron Microscopy Sciences, Hatfield, PA). SERS mapping was carried out at the multiplex Raman peak at 1120 cm^{-1} (Cy5) for TGFβRII, 1175 cm^{-1} (MGITC) for CD44 and 1650 cm^{-1} (Rh6G) for EGFR biomarker using streamline mapping scans with 1 μm steps size over the specified area with an integration time of 1 second.

***In vivo* SERS measurement.** Balb/c nude female mice (6–8 weeks old) obtained from the Biological Resource Centre (Biomedical Sciences Institute, A*STAR) were inoculated subcutaneously on the right flank with 5×10^6 MDA-MB-231 cells mixed in 1 : 1 ratio with Matrigel (BD Biosciences) in a volume of 200 μL . After 2 weeks, when the tumors grew to a palpable size, 200 μL of the mixture of antibody conjugated (test formulation) and non-antibody conjugated (control formulation) SERS nanotags were injected into the centre of the tumor location. *In vivo* SERS measurements were performed at a minimum of six locations (at and around injected site on the tumor) at different depths. At each location, spectra were acquired thrice on tumor site, liver and spleen using 30 mW, 785 nm laser excitation through a 20 \times objective lens (Leica, NA 0.40). Same lens was used to collect the Stokes shifted Raman signal. All animal experimental procedures were performed in accordance with protocol #120774 approved by the Institutional Animal Care and Use Committee (IACUC).

1. Kang, H. *et al.* Near-infrared SERS nanoprobe with plasmonic Au/Ag hollow-shell assemblies for *in vivo* multiplex detection. *Adv. Funct. Mater.* **23**, 3719–3727 (2013).



2. Kho, K. W., Fu, C. Y., Dinish, U. S. & Olivo, M. Clinical SERS: are we there yet? *J Biophotonics*. **4**, 667–684 (2011).
3. Zhang, Y., Hong, H., Myklejord, D. V. & Cai, W. Molecular imaging with SERS-active nanoparticles. *Small*. **7**, 3261–3269 (2011).
4. Xie, W. & Schlucker, S. Medical applications of surface-enhanced Raman scattering. *Phys.Chem. Chem. Phys.* **15**, 5329–5344 (2013).
5. Bantz, K. C. *et al.* Recent progress in SERS biosensing. *Phys. Chem. Chem. Phys.* **13**, 11551–11567 (2011).
6. Lee, S. *et al.* Biological imaging of HEK293 cells expressing PLC gamma1 using surface-enhanced Raman microscopy. *Anal Chem.* **79**, 916–922 (2007).
7. Faulds, K., Barbagallo, R. P., Keer, J. T., Smith, W. E. & Graham, D. SERS as a more sensitive technique for the detection of labelled oligonucleotides compared to fluorescence. *Analyst*. **129**, 567–568 (2004).
8. Woo, M. A. *et al.* Multiplex immunoassay using fluorescent-surface enhanced Raman spectroscopic dots for the detection of bronchioalveolar stem cells in murine lung. *Anal. Chem.* **81**, 1008–1015 (2009).
9. Zavaleta, C. L. *et al.* Multiplexed imaging of surface enhanced Raman scattering nanotags in living mice using noninvasive Raman spectroscopy. *Proc. Natl. Acad. Sci. U. S. A.* **106**, 13511–13516 (2009).
10. Maiti, K. K. *et al.* Multiplex targeted *in vivo* cancer detection using sensitive near-infrared SERS nanotags. *Nano Today*. **7**, 85–93 (2012).
11. Dougan, J. A. & Faulds, K. Surface enhanced Raman scattering for multiplexed detection. *Analyst*. **137**, 545–554 (2012).
12. Dinish, U. S., Balasundaram, G., Chang, Y. T. & Olivo, M. Sensitive multiplex detection of serological liver cancer biomarkers using SERS-active photonic crystal fiber probe. *J. Biophotonics*. 1–10, DOI 10.1002/jbio.201300084 (2013).
13. Keren, S. *et al.* Noninvasive molecular imaging of small living subjects using Raman spectroscopy. *Proc. Natl. Acad. Sci. U.S.A.* **105**, 5844–5849 (2008).
14. Qian, X. *et al.* *In vivo* tumor targeting and spectroscopic detection with surface enhanced Raman nanoparticle tags. *Nat. Biotechnol.* **26**, 83–90 (2008).
15. Maiti, K. K. *et al.* Development of biocompatible SERS nanotag with increased stability by chemisorption of reporter molecule for *in vivo* cancer detection. *Biosens. Bioelectron.* **26**, 398–403 (2010).
16. Samanta, A. *et al.* Ultrasensitive near-infrared Raman reporters for SERS-based *in vivo* cancer detection. *Angew. Chem. Int. Ed.* **50**, 6089–6092 (2011).
17. Kustner, B. *et al.* SERS labels for red laser excitation: silica-encapsulated SAMs on tunable gold/silver nanoshells. *Angew. Chem. Int. Ed.* **48**, 1950–1953 (2009).
18. Han, M., Gao, X., Su, J. Z. & Nie, S. Quantum-dot-tagged microbeads for multiplexed optical coding of biomolecules. *Nat. Biotechnol.* **19**, 631–635 (2001).
19. Van Sark, M. H. J. G. W. *et al.* Photooxidation and photobleaching of single CdSe/ZnS quantum dots probed by room-temperature time-resolved spectroscopy. *J. Phys. Chem. B.* **105**, 8281–8284 (2001).
20. Von Maltzahn, G. *et al.* SERS-coded gold nanorods as a multifunctional platform for densely multiplexed near-infrared imaging and photothermal heating. *Adv. Mater.* **21**, 3175–3180 (2009).
21. Qian, J., Jiang, L., Cai, F., Wang, D. & He, S. Fluorescence-surface enhanced Raman scattering co-functionalized gold nanorods as near-infrared probes for purely optical *in vivo* imaging. *Biomaterials*. **32**, 1601–1610 (2011).
22. Wu, L. *et al.* Simultaneous evaluation of p53 and p21 expression level for early cancer diagnosis using SERS technique. *Analyst*. **138**, 3450–3456 (2013).
23. Sanles-Sobrido, M. *et al.* Design of SERS-encoded, submicron, hollow particles through confined growth of encapsulated metal nanoparticles. *J. Am. Chem. Soc.* **131**, 2699–2705 (2009).
24. Lee, S. *et al.* Surface-enhanced Raman scattering imaging of HER2 cancer markers overexpressed in single MCF7 cells using antibody conjugated hollow gold nanospheres. *Biosens. Bioelectron.* **24**, 2260–2263 (2009).
25. Yuan, H. *et al.* Quantitative surface-enhanced resonant Raman scattering multiplexing of biocompatible gold nanostars for *in vitro* and *ex vivo* detection. *Anal. Chem.* **85**, 208–212 (2013).
26. Xie, J., Zhang, Q., Lee, J. & Wang, D. The synthesis of SERS-active gold nanoflower tags for *in vivo* applications. *ACS Nano*. **2**, 2473–2480 (2008).
27. Vendrell, M., Maiti, K. K., Dhaliwal, K. & Chang, Y. T. Surface-enhanced Raman scattering in cancer detection and imaging. *Trends. Biotechnol.* **31**, 249–257 (2013).
28. Wang, X. *et al.* Detection of circulating tumor cells in human peripheral blood using surface-enhanced Raman scattering nanoparticles. *Cancer. Res.* **71**, 526–1532 (2011).
29. Chen, Y. *et al.* Immunoassay for LMP1 in nasopharyngeal tissue based on surface-enhanced Raman scattering. *Int J Nanomedicine*. **7**, 73–82 (2012).
30. Wang, H. N. & Vo-Dinh, T. Multiplex detection of breast cancer biomarkers using plasmonic molecular sentinel nanoprobe. *Nanotechnology*. **20**, 065101 (1–6) (2009).
31. Matschulat, A., Drescher, D. & Kneipp, J. Surface-enhanced Raman scattering hybrid nanoprobe multiplexing and imaging in biological systems. *ACS Nano*. **4**, 3259–3269 (2010).
32. Wang, Y., Seebald, J. L., Szeto, D. L. & Irudayaraj, J. Biocompatibility and biodistribution of surface-enhanced Raman scattering nanoprobe in zebrafish embryos: *in vivo* and multiplex imaging. *ACS Nano*. **4**, 4039–4053 (2010).
33. McVeigh, P. Z., Mallia, R. J., Veilleux, I. & Wilson, B. C. Wide field quantitative multiplex surface enhanced Raman scattering imaging *in vivo*. *J. Biomed. Opt.* **18**, 046011-1-046011-8 (2013).
34. Zavaleta, C. L. *et al.* A Raman-based endoscopic strategy for multiplexed molecular imaging. *Proc. Natl. Acad. Sci. U. S. A.* **110**, E2288–2297 (2013).
35. Tsutsui, S. *et al.* Prognostic and predictive value of epidermal growth factor receptor in recurrent breast cancer. *Clin Cancer Res.* **8**, 3454–3460 (2002).
36. Hiraga, T., Ito, S. & Nakamura, H. Cancer stem-like cell marker cd44 promotes bone metastases by enhancing tumorigenicity, cell motility and hyaluronan production. *Cancer Res.* **73**, 4112–4122 (2013).
37. Bacman, D. *et al.* TGF-beta receptor 2 down regulation in tumour-associated stroma worsens prognosis and high-grade tumours show more tumour-associated macrophages and lower TGF-beta1 expression in colon carcinoma: a retrospective study. *BMC Cancer*. **7**, 156, doi:10.1186/1471-2407-7-156 (2007).
38. Brincker, H. Direct intratumoral chemotherapy. *CritRev Oncol Hematol.* **15**, 91–98 (1993).
39. Walter, K. A., Tamargo, R. J., Olivi, A., Burger, P. C. & Brem, H. Intratumoral chemotherapy. *Neurosurgery*. **37**, 1128–1145 (1995).
40. Voulgaris, S. *et al.* Intratumoral doxorubicin in patients with malignant brain gliomas. *Am J ClinOncol.* **1**, 60–64 (2002).
41. Goldberg, E. P., Hadba, A. R., Almond, B. A. & Marotta, J. S. Intratumoral cancer chemotherapy and immunotherapy: opportunities for nonsystemic preoperative drug delivery. *J Pharm Pharmacol.* **54**, 159–180 (2002).
42. Duvillard, C., Romanet, P., Cosmidis, A., Beaudouin, N. & Chauffert, B. Phase 2 study of intratumoral cisplatin and epinephrine treatment for locally recurrent head and neck tumors. *Ann Otol Rhinol Laryngol.* **113**, 229–233 (2004).
43. Lammers, T. *et al.* Effect of intratumoral injection on the biodistribution and the therapeutic potential of HPMA copolymer-based drug delivery systems. *Neoplasia*. **8**, 788–795 (2006).
44. Yang, L. *et al.* Single chain epidermal growth factor receptor antibody conjugated nanoparticles for *in vivo* tumor targeting and imaging. *Small*. **5**, 235–243 (2009).
45. Kong, K. V., Lam, Z., Goh, W. D., Leong, W. K. & Olivo, M. Metal carbonyl-gold nanoparticle conjugates for live-cell SERS imaging. *Angew. Chem. Int. Ed.* **51**, 9796–9799 (2012).
46. Dinish, U. S. *et al.* Highly sensitive SERS detection of cancer proteins in low sample volume using hollow core photonic crystal fiber. *Biosens. Bioelectron.* **33**, 293–298 (2012).
47. Maiti, K. K. *et al.* Multiplex cancer cell detection by SERS nanotags with cyanine and triphenylmethine Raman reporters. *Chem Comm.* **47**, 3514–3516 (2011).
48. Lampidis, T. J., Hasin, Y., Weiss, M. J. & Chen, L. B. Selective killing of carcinoma cells “*in vitro*” by lipophilic-cationic compounds: a cellular basis. *Biomed Pharmacother.* **39**, 220–226 (1985).
49. Sonavane, G., Tomoda, K. & Makino, K. Biodistribution of colloidal gold nanoparticles after intravenous administration: effect of particle size. *Colloids Surf B Biointerfaces.* **66**, 274–280 (2008).
50. Xie, H., Goins, B., Bao, A., Wang, Z. J. & Phillips, W. T. Effect of intratumoral administration on biodistribution of 64Cu-labeled nanoshells. *Int. J Nanomedicine.* **7**, 2227–2238 (2012).
51. Yong, K. T., Roy, I., Ding, H., Bergery, E. J. & Prasad, P. N. Biocompatible near-infrared quantum dots as ultrasensitive probes for long-term *in vivo* imaging applications. *Small*. **5**, 1997–2004 (2009).
52. Hong, W. S. & Hong, S. I. Clinical usefulness of alpha-1-antitrypsin in the diagnosis of hepatocellular carcinoma. *J. Korean Med Sci.* **6**, 206–213 (1991).
53. Waldmann, T. A. & McIntire, K. R. The use of a radioimmunoassay for alpha-fetoprotein in the diagnosis of malignancy. *Cancer*. **34**, 1510–1515 (1974).

Acknowledgments

Authors would like to thank Mr. Jason Soh (BOIG, SBIC, A*STAR, Singapore) for his help in TEM measurements and Dr. Amalina Attia (BOIG, SBIC, A*STAR, Singapore) for the fruitful discussion.

Author contributions

D.U.S., G.B. and M.O. designed the research. D.U.S. and G.B. carried out the experiments and revised the manuscript. C.Y.T. synthesized one of the Raman reporter molecules. D.U.S., G.B. and M.O. analysed data and wrote the manuscript. M.O. oversaw the study and supervised the project. All authors reviewed the manuscript.

Additional information

Supplementary information accompanies this paper at <http://www.nature.com/scientificreports>

Competing financial interests: The authors declare no competing financial interests.

How to cite this article: Dinish, U.S., Balasundaram, G., Chang, Y.-T. & Olivo, M. Actively Targeted *In Vivo* Multiplex Detection of Intrinsic Cancer Biomarkers Using Biocompatible SERS Nanotags. *Sci. Rep.* **4**, 4075; DOI:10.1038/srep04075 (2014).



This work is licensed under a Creative Commons Attribution-NonCommercial-ShareAlike 3.0 Unported license. To view a copy of this license, visit <http://creativecommons.org/licenses/by-nc-sa/3.0>